J. Phys. Chem. Solids Pergamon Press 1971. Vol. 32, pp. 1707–1720. Printed in Great Britain.

DRIFT VELOCITY OF ELECTRONS AND HOLES AND ASSOCIATED ANISOTROPIC EFFECTS IN SILICON*

C. CANALI, G. OTTAVIANI and A. ALBERIGI QUARANTA
Istituto di Fisica, Università di Modena, Via Vivaldi 70, Modena, Italy

(*Received* 10 *August* 1970; *in revised form* 23 *November* 1970)

Abstract—The drift velocity of electrons and holes in high purity silicon has been measured, with the time of flight technique, as a function of electric field (0·1–50 KV/cm) at several temperatures between 77 and 300°K. By applying the electric field parallel to the ⟨111⟩ and ⟨100⟩ crystallographic directions, an evident longitudinal anisotropy effect has been found for the drift velocity of electrons and also, for the first time, for the drift velocity of holes. At high values of the electric field a saturation drift has been found for the electrons at the temperatures considered in these experiments. On the contrary, no saturation has been attained for holes, even at the highest applied electric fields. The ohmic mobility has been measured between 77 and 300°K for electrons and between 160 and 300°K for holes. When a comparison is possible, our results are in good agreement with other experimental results found in the literature. A qualitative theoretical interpretation of the effects observed is given.

1. INTRODUCTION

SILICON is the most studied and widely employed semiconductor. The problem of the charge transport in low and high fields has been studied since the early 50's [1–25].

However the drift velocity of the charge carriers under non ohmic conditions as a function of the electric field, the crystal axis orientation, and the temperature is little known in the 300–77°K range (almost no data exist for holes) and practically unknown at temperatures below 77°K. In most of the previous papers [5, 9–18] the values of the charge carrier mobility were obtained by indirect measurements (microwaves absorption, conductivity, space charge limited current) based on incompletely verified assumptions and on inexactly known parameters. Therefore we have made a very accurate series of measurements by a technique which, because of its absolute nature (the drift velocity is obtained by simply dividing the distance travelled by the time employed), should ensure the validity of the results obtained within the experimental errors. A first series of results is presented here, covering the 300–77°K temperature range for fields of 0·1–50 KV/cm and for two crystallographic directions; in a later paper we hope to present data for the temperature range below 77°K.

Our most interesting new results are (a) the finding of a clear anisotropy effect in the hot hole drift along the ⟨111⟩ and ⟨100⟩ crystallographic directions, and (b) the determination of the electron saturation drift at different temperatures.

After a short description of the experimental technique, the results obtained are reported and discussed, and when possible, compared with those given in the literature.

2. THE TIME OF FLIGHT TECHNIQUE

Although for many years it was not considered a classical technique by solid state physicists, the time of flight technique has turned out to be one of the most effective in studying carrier transport properties (drift velocity, trapping, etc.) of semiconductors. In order to clarify our experimental results, the principles of the time of flight technique and some of its features are briefly described.

*Partially supported by Consiglio Nazionale delle Ricerche, Italy.

The time of flight technique[19–25] is based on the analysis of the current signal induced by the transport of charge carriers in a region of uniform electric field that extends across a sample of known width W.

If the charge carriers are created by an ionizing radiation with a range R which is shorter than the sample width W (Fig. 1), the carriers of one type are collected after having travelled a negligible fraction of W, while the carriers of the other type have to drift across the whole sample with a velocity v_d and are collected at the opposite electrode after a time $T_R = W/v_d$. In this case the shape of the current signal induced at the ends of the space charge region is determined only by the motion of the carriers which drift across the entire width W[20, 26], and it is given by

$$i(t) = \frac{Nqv_d}{W} u(t - T_R) \qquad (1)$$

where N is the number of carriers (electrons or holes) created by the radiation, q is the electron charge, and

$$u(t-T_R) = \begin{cases} 1 \text{ for } 0 \leq t \leq T_R \\ 0 \text{ for } t > T_R \text{ and } t < 0. \end{cases}$$

The time duration of this signal is equal to the transit time T_R and it depends upon the time necessary for only one kind of charge carriers to travel the distance W. Thus, the time of flight technique permits the investigation, separately, of the transport coefficients of both types of carriers in the same sample.

To measure the drift velocity of electrons and holes in silicon we used surface barrier devices obtained by evaporating a thin gold layer ($< 10^3$ Å) on to the high resistivity silicon wafer. The back contact was a thin evaportated aluminum layer ($< 10^3$ Å).

In our measurements the diodes are inversely biased with a voltage V_A larger than the so-called total depletion voltage V_0, defined as the voltage necessary for the space charge region to occupy the whole thickness of the sample. The values of V_A were large enough to ensure a practically constant electric field in the samples.

In the first case shown in Fig. 1 an ionizing radiation produces a cloud of electron-hole pairs near the gold contact; the current signal is then due only to the electron flight. On the contrary, if the pairs of charge carriers are created on the opposite side of the space charge region (Al contact), the current signal is due only to the hole motion.

This experimental method has the following advantages over the techniques generally used to investigate transport properties in semiconductors: it provides a direct measurement

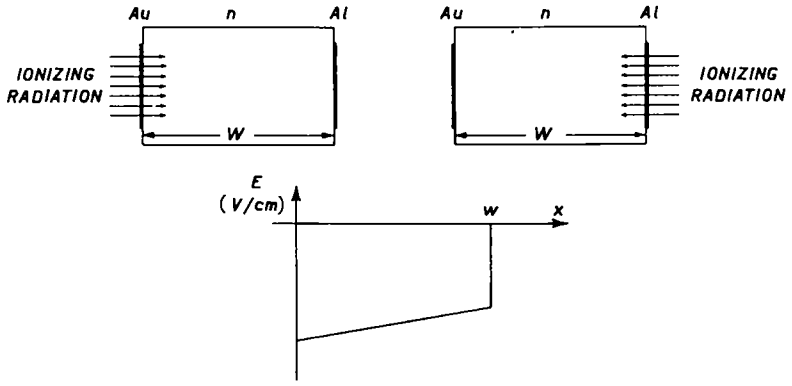

Fig. 1. Schematic view of the ionizing radiation impinging on a surface barrier diode near the Au–Si contact or the Al–Si contact. Also shown is the electric field profile inside the space charge region $V_a > V_0$.

of the drift velocity of the carriers as a function of electric field; it permits investigation of the motion of both electrons and holes in the same sample; it is based entirely on a bulk phenomenon and therefore avoids the difficulties associated with the more traditional techniques, related to surface effects, contact injection, and equivalent circuit of the device; it can be used for drift velocity measurements with high applied electric fields without heating effects, since the current flowing through the device is always very low because of the inverse bias of the junction and the dissipated power is always within a few mW; it is applicable only to samples with very low concentrations of ionized impurities and therefore is the most suitable method for measuring drift velocities as functions of electric field at very low temperatures or in semi-insulating materials; it is not affected by multiplication or secondary ionization phenomena; under suitable experimental conditions it is not affected by the presence of space charge distribution[27, 28], which could vary the field profile inside the sample; under certain conditions, discussed below, it can be used for drift velocity measurements also in the presence of trapping[29].

3. DISCUSSION OF THE TECHNIQUE

(a) *Electric field*

The interpretation of the experimental data is based on the assumption that the electric field is constant inside the region W. In general this is not true in a surface barrier diode, where the electric field is a linear function of x in the space charge region (see Fig. 1). In this case the $v_d(E)$ relation must be obtained from calculation of the time of flight $T_0 = \int_0^W dx/v_d E(x)$. This calculation can be performed by an iterative method. We have avoided this complication by using samples with very high resistivity. In fact the choice of a sample material with a very low impurity concentration diminishes the slope of the electric field inside the space charge region. Moreover, the choice of a thin junction decreases the effect of electric field variations inside the junction. The error in the transit time measurements due to assumption of a constant electric field rather than use of its real value is given by:

$$\frac{T_0 - T_R}{T_R} = \frac{E_0}{E_1} \ln \frac{1 + \frac{1}{2}\frac{E_1}{E_0}}{1 - \frac{1}{2}\frac{E_1}{E_0}} - 1$$

where T_R and T_0 are the transit times respectively with a constant and a linearly varying electric field*, E_0 is the average value of the electric field, and E_1 is the difference between the values of the electric field at the junction (Au) and at the ohmic contact (Al) ($E_1 = 2 V_0/W$).

In all cases considered in our experiment the error $(T_R - T_0)/T_0$ was less than 2 per cent.

(b) *Space charge effects*

In order to perform drift velocity measurements, particularly in the low field region, the number of carriers created by the ionizing radiation must be large enough to produce a measurable current signal (cf. equation (1)), but not so large as to perturb the electric field inside the device. Such a perturbation would cause an increase in the charge collection time and therefore a fictitious decrease in the mobility. This effect[27, 28] decreases at lower temperatures, higher electric fields, and lower carrier concentrations.

The absence of such a perturbation under our experimental conditions has been both determined theoretically, by solving the charge transport equations in the space charge region, and confirmed experimentally, by varying the density of the e–h pairs without any appreciable effect on the shape and duration of the current signal.

*A quantitative treatment of this problem has been published[20, 21].

(c) *Equivalent circuit effect*

The effect of the equivalent circuit of the device can be easily evaluated under our operation conditions by taking into account that the diode behaves as a pure capacity C [20]. The current signal displayed by a sampling oscilloscope with an input impedance $R_0 = 50\,\Omega$ therefore has a risetime approximately equal to $2{\cdot}2\,R_0C$. We have chosen the effective areas of the diodes, particularly in the thinnest samples, in such a way that this risetime does not introduce an error greater than 2 per cent in the measured duration of the current signal. This duration depends only upon the drift velocity of the carriers and is practically unaffected by their diffusion [30].

(d) *Trapping*

The determination of the transit time by means of the analysis of the current signal induced by the charge carriers at contacts of the sample can be affected by trapping phenomena. A phenomenological theory of this effect [29] shows that practically the true value of the transit time T_R is obtained by measuring if $T_R \approx \tau^+$, where τ^+ is the mean free drift time of the carriers.

In the worst case in our measurements $T_R \approx 5\ 10^{-8}$ sec, and the value of τ^+ is

$$\tau^+ = \frac{1}{\sigma N_T v_{th}} = 10^{-6}\,\text{sec}$$

where $\sigma (< 10^{-13}\,\text{cm}^{-2})$ [31] is the capture cross section of the traps, $N_T (< 10^{12}\,\text{cm}^{-3})$ is the trapping center concentration, and $v_{th} (\approx 10^7\,\text{cm/sec})$ is the thermal velocity of the charge carriers.

4. EXPERIMENTAL APPARATUS

Figure 2 is a block diagram of the experimental apparatus. The ionizing radiation consists of bursts of 40 keV electrons. The duration of the bursts is $\approx$70 ps and their repetition rate may be varied. The number of electrons in each burst can be as high as 10^4. They are produced by an electron gun [32], and their range in silicon is about 7 μm. This electron accelerator permits control of the number and the density of the pairs created in the sample. Furthermore, it provides a reference time signal related to the arrival of the electron burst on the sample. This signal allows application of pulsed rather than continuous bias voltages to the samples so that higher fields may be applied and heating

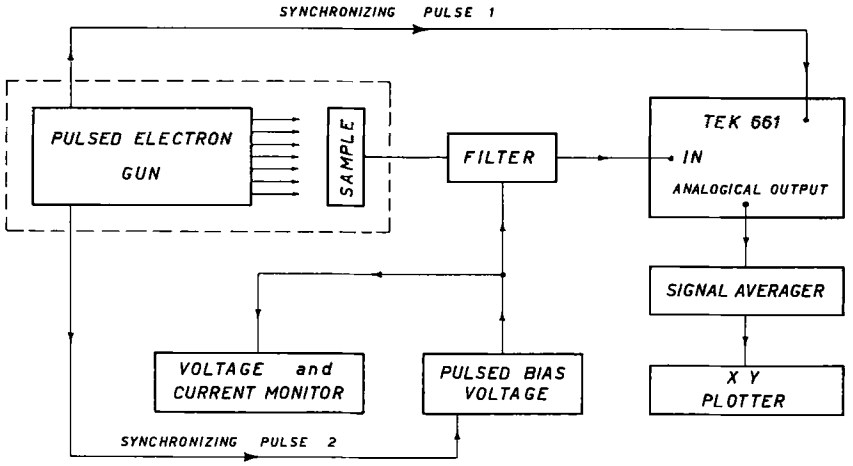

Fig. 2. Block diagram of the experimental setup.

effects, especially at high fields, may be avoided.

The surface barrier diodes are enclosed in a vacuum chamber and can be cooled down to 77°K.

The current signal produced by each burst is sent directly by means of a 50 ohm coaxial cable to a sampling oscilloscope. The geometry and the setup of the sample minimize parasitic capacities and inductances; therefore, the total risetime of the electronic apparatus is less than 100 ps. The current signal recorded by the sampling oscilloscope is sent from the analogic output of the oscilloscope to an XY plotter. When the signal/noise ratio is too low a Signal Averaging Computer (Nuclear Data mod. ND 801) is put between the output and the plotter.

A typical example of a signal recorded by the plotter is shown in Fig. 3. The transit time T_R of the carriers is determined by measuring the full width half maximum of the current signal. A careful examination of the equivalent circuit of the junction (see below) confirmed that, under the bias conditions ($V_A > V_0$) employed in the experiment, the measured values of the transit time depend only upon the drift velocity of the carriers.

The diodes are made of high purity, high resistivity (30–200 $K\Omega$-cm at room temperature) n-type silicon monocrystal wafers cut perpendicularly to the ⟨111⟩ and ⟨100⟩ crystallographic directions.

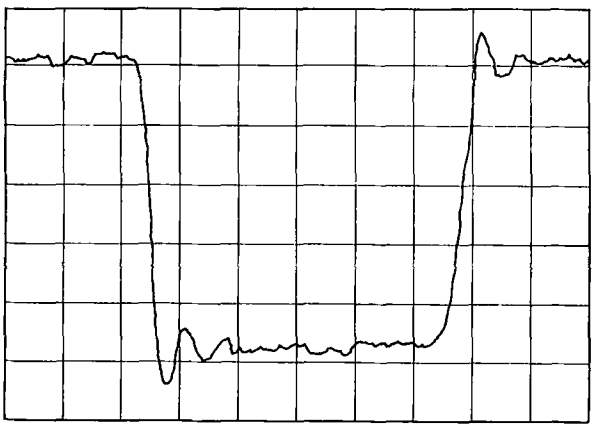

Fig. 3. Typical waveform of the current signal due to electron transport at 300°K. The width of the diode is 500 μm, and the applied voltage is 1250 V. The drift velocity obtained from this signal is $9{\cdot}23 \times 10^6$ cm/sec. Horizontal Sensitivity 1 ns./division.

All crystals are characterized by high carrier lifetimes (> 3000 μs) and a low concentration of dislocations: EPD < 15000 cm^{-2}.

The thicknesses of the detectors are between 100 and 600 μm and have been measured with a precision of the order of 1 per cent. Their effective areas are between 4 and 15 mm^2.

All the devices can be cooled down to 77°K, and bias voltages much higher than the total depletion voltage can be applied.

5. EXPERIMENTAL RESULTS

We have measured the drift velocity of charge carriers (electrons and holes) in high purity silicon, varying the electric field between 0·1 and 50 KV/cm and the temperature between 77 and 300°K.

The measurements were made on 24 samples, 13 oriented in the ⟨111⟩ crystallographic direction and 11 in the ⟨100⟩ direction. The final data are the result of the analysis of about 10^4 graphs.

Most of the samples were prepared in our laboratory with high purity, high resistivity n-type silicon supplied by Wacker Chemitronic, but a few samples were made with silicon produced by Holder Topsöe and by Hoboken. Some pairs of samples oriented along the ⟨111⟩ and ⟨100⟩ directions were obtained from the same ingots.

With the technique used it was possible to measure the drift velocity of both electrons and holes in the same sample. By means of the pulsed electron accelerator we could vary the density of the e–h pairs to avoid space charge limited current effects. Finally, the repetition rate of the bias signal in the diode was varied in order to avoid heating effects at high electric fields.

In order to cover the largest possible range of electric fields while maintaining the experimental conditions discussed above, we made

measurements on samples with different resistivities, thicknesses, and useful surfaces. The experimental results obtained with different samples were always in excellent agreement.

Figure 4 shows a typical set of electron drift velocity data along a ⟨111⟩ crystallographic direction at 300°K, obtained with 13 different samples not separately identified in the figure. The spread of the experimental data was not more than 5 per cent.

For clarity, only the best fits of the experimental data are shown in the following figures.

(a) *Electrons*

Figure 5 shows the results obtained for the drift velocity of the electrons as a function of the electric field, applied parallel to the ⟨111⟩ crystallographic direction, at several temperatures.

Figures 6a, b and c show the longitudinal anisotropy of the electron drift when the electric field is applied along a ⟨111⟩ or a ⟨100⟩ direction.

As seen from Figs. 5 and 6, v_d has been measured from the ohmic region up to the saturation value*. The results obtained for the ohmic mobilities (the same for all crystallographic directions) for several temperatures are shown in Table 1, along with data available in the literature.

Figure 5 shows, as already known[39], that the electron mobility is no longer ohmic for electric fields higher than a certain critical value. It also shows that when the lattice temperature is decreased, the carriers are 'heated up' above the lattice thermal energy at lower applied electric fields because of the higher mobility of the carriers and the lower efficiencies of the scattering mechanisms.

The longitudinal anisotropy of the carrier drift velocity along the ⟨111⟩ and ⟨100⟩ directions can be qualitatively understood by taking into account the band structure of silicon and the scattering mechanisms which mix different valleys: when the electric field E is applied parallel to a ⟨111⟩ direction, all

*Saturation drift velocity is that value of v_d which does not change, within the experimental errors, in a large interval of electric fields (for instance between 14 and 28 KV/cm at 77°K) at a given temperature.

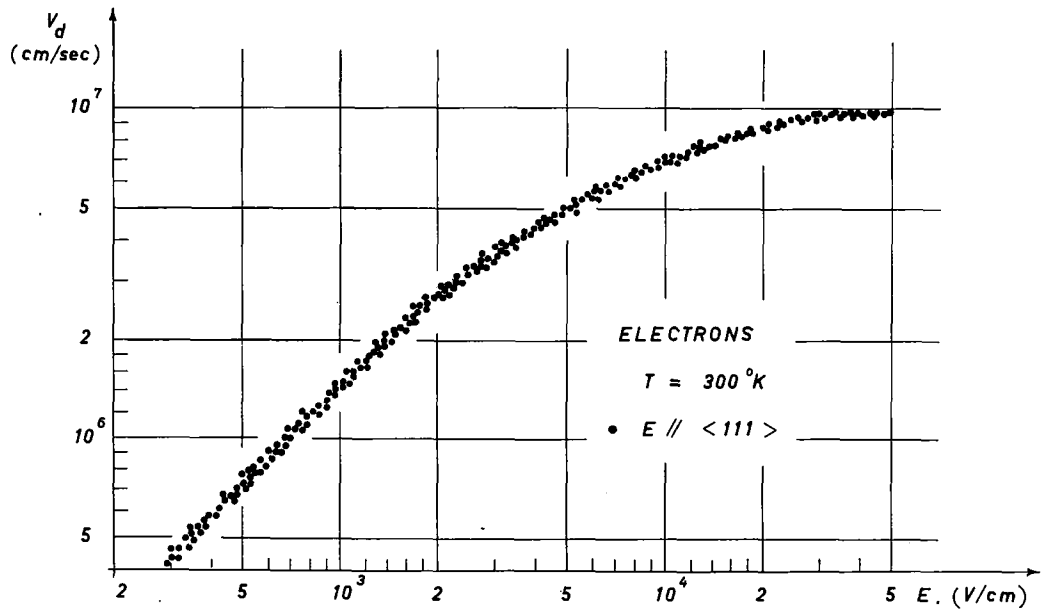

Fig. 4. A typical set of experimental results obtained on 13 different samples.

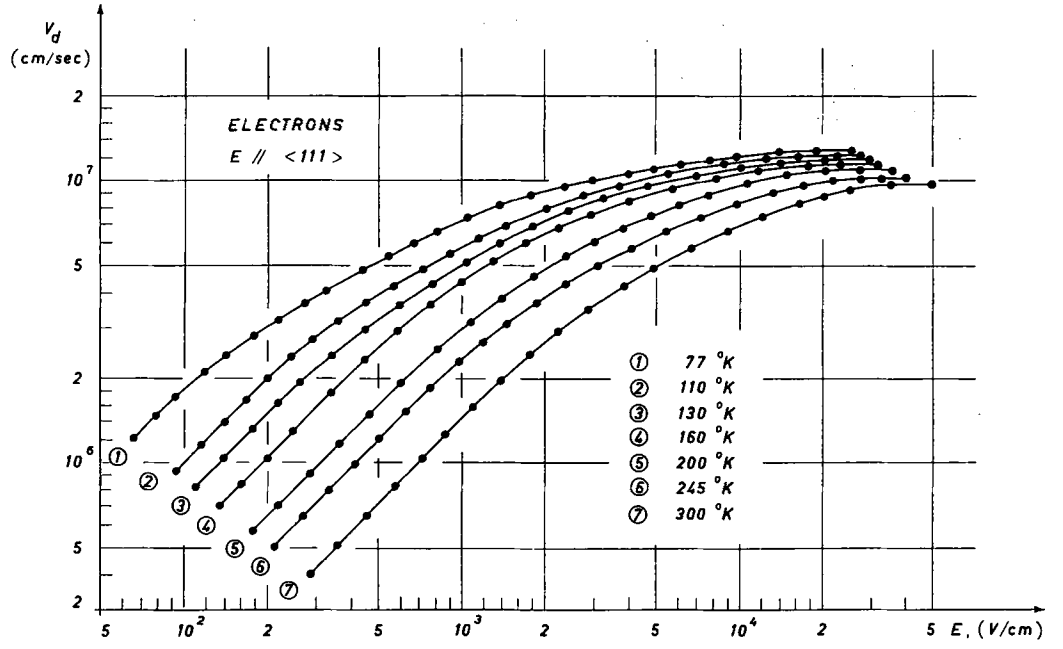

Fig. 5. Electron drift velocity as a function of the electric field parallel to the ⟨111⟩ crystallographic direction at several temperatures.

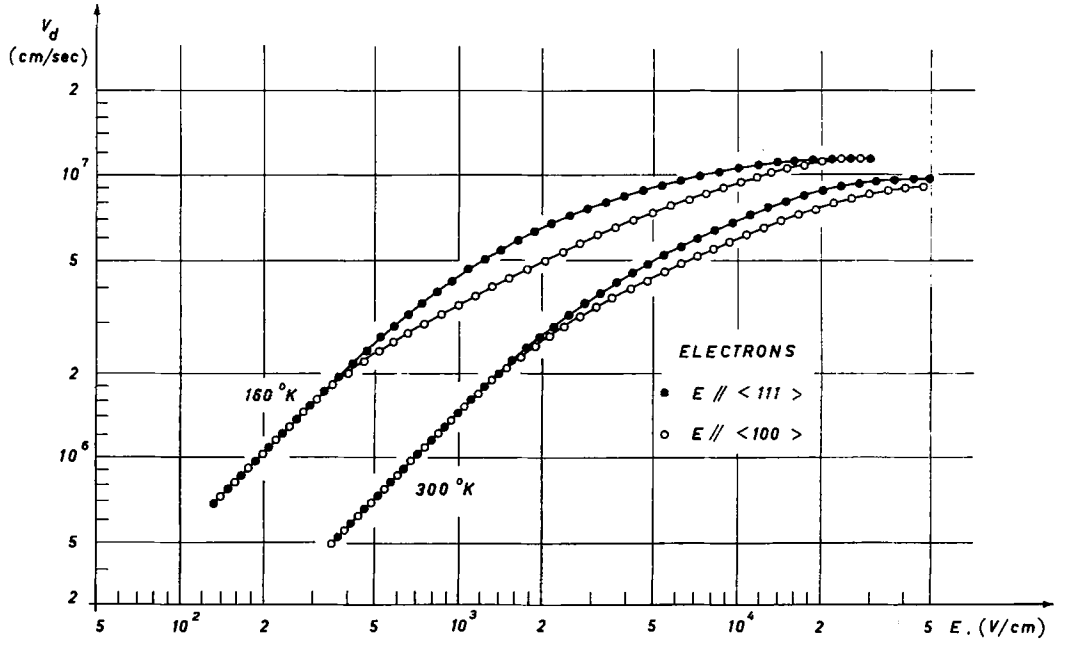

Fig. 6(a)

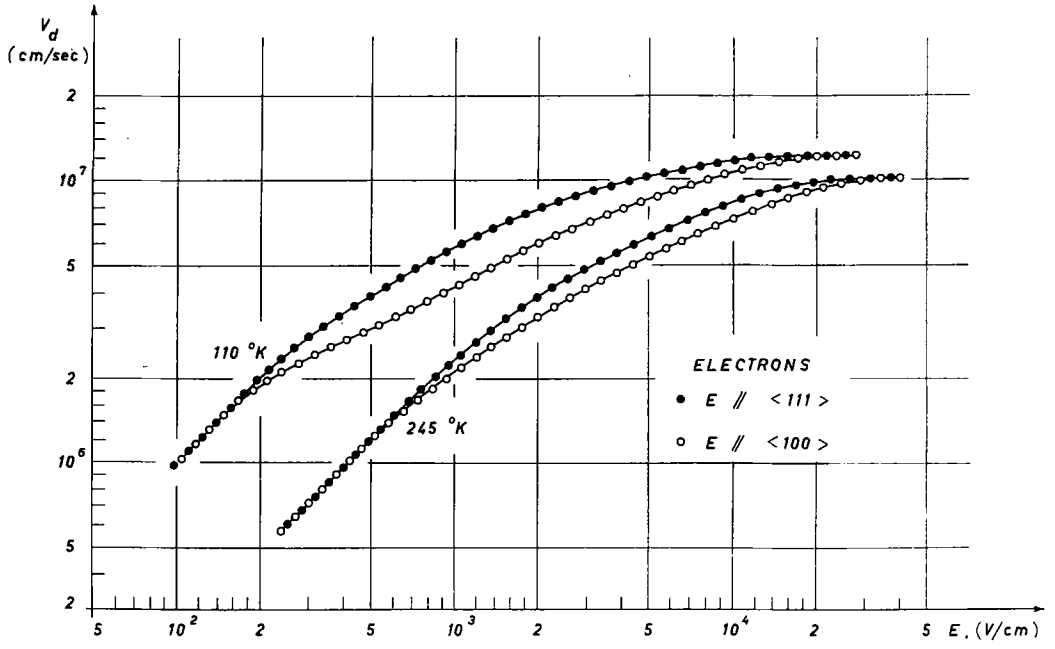

Fig. 6(b)

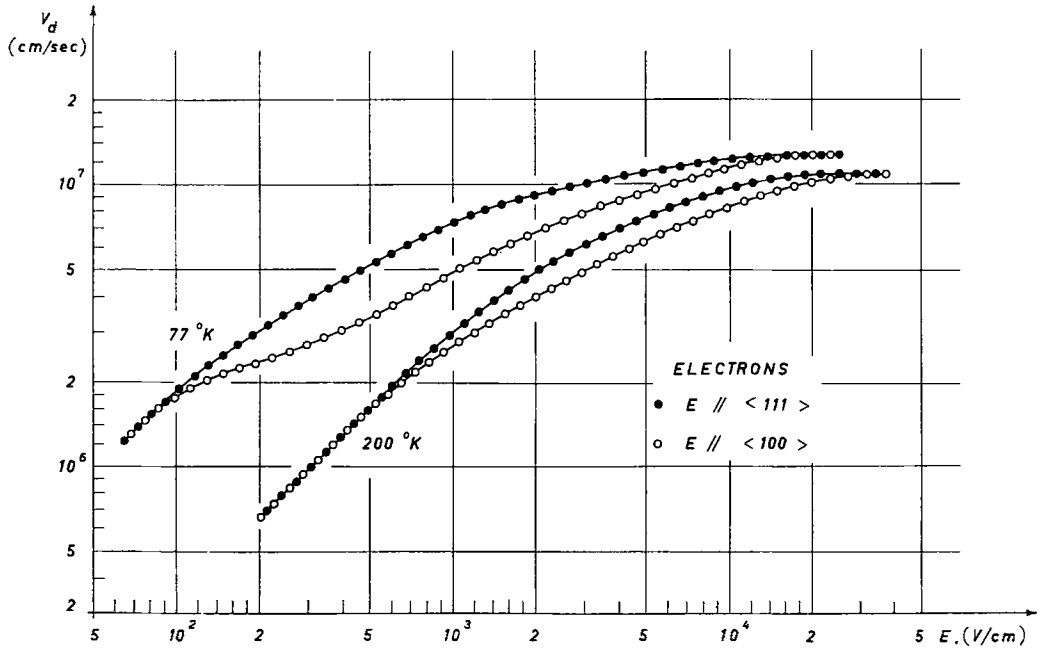

Fig. 6(c)

Figs. 6(a) (b) and (c). Electron drift velocities as functions of the electric field parallel to the ⟨111⟩ and ⟨100⟩ directions, at several temperatures.

Table 1. Our values of electron ohmic mobility at various temperatures compared with the results of others. (Reference numbers in brackets)

T °K	Our results	$\mu(cm^2V^{-1}sec^{-1})$				
		1500				
300	1450	1200 ± 100 [33]	1450 [7]	1350 ± 100 [37]	1450 [34]	1318 [38]
245	2400	2350 [36]				1888 [38]
200	3250	3850 [34]	4000 [35]	2600 [9]		2740 [38]
160	5200	6000 [36]				4230 [38]
130	7500	7600 [36]	6500 [9]			6490 [38]
110	10000	10600 [36]				9175 [38]
77	20000	20000 [35, 16]	27000 [34]	11000 [9]		22000 [38]

the six ⟨100⟩ valleys are oriented alike with respect to E. They all exhibit the same behaviour and therefore give the same contribution to the transport properties of the sample. On the contrary, when E is applied parallel to the ⟨100⟩ direction, the two valleys ⟨100⟩ and ⟨$\bar{1}$00⟩ have their longitudinal axes parallel to the electric field, so that they have states populated predominantly along these axes, characterized by a larger effective mass ($0{\cdot}9\,m_0$, where m_0 is the free electron mass), but the remaining four valleys, whose longitudinal axes are oriented perpendicularly to the field, are characterized by electrons having a lower effective mass ($0{\cdot}2\,m_0$). Lighter electrons are more easily accelerated and thus heated up by the field. Unless the electron concentration is so high that the electron–electron collisions tend to equalize all mean energies of the valleys, the lighter electrons should attain a higher mean energy than the heavier ones. Accordingly the four perpendicular valleys are called 'hot' and the two longitudinal valleys 'cold'. In this case the two parallel valleys (cold) exhibit a lower mobility, and the four perpendicular valleys (hot) a higher mobility.

However, since the presence of intervalley scattering enhances the number of electrons in the cold valleys more than in the hot ones, the overall effect is a final lower drift velocity when the applied electric field is parallel to the ⟨100⟩ direction than when it is parallel to the ⟨111⟩.

The anisotropic effect is temperature dependent (Figs. 6) because of the population shift from hotter to colder valleys [39]. With increasing lattice temperature this shift is enhanced, and consequently the anisotropy is less. On the other hand, when the applied electric field is so high that electrons in colder valleys are also energetic enough to emit intervalley phonons, the two processes – from cold to hot and from hot to cold – are nearly equalized, and the drift velocities in the two directions ⟨111⟩ and ⟨100⟩ tend to reach the same value and exhibit a saturation velocity. This saturation value (as seen in Figs. 6) is the same for both the ⟨111⟩ and ⟨100⟩ crystallographic directions at all temperatures, except at 300°K, where at the highest applied electric field a small anisotropy effect is still present. The drift velocity saturation may be understood by taking into account the non parabolicity of the conduction band [40] and the possible electron–phonon interactions which are forbidden at low fields [41, 42].

In Table 2 our experimental data on the saturation drift velocity are compared with the results of others*. The discrepancies can be justified by the following considerations: Our measurement is an absolute one, in contrast to that obtained with the method used by Rodriguez and Nicolet [43].

*Preliminary measurements of the saturation drift have been made on two samples in the temperature range between 4·2 and 77°K [44].

Table 2. Limiting values of the electron drift velocity at various temperatures. Other values obtained at 300°K *are:* 9 10^6 cm/sec, *Zulliger et al.*[22]; 10^7 cm/sec, *Norris and Gibbons*[21]; 9·2 10^6 cm/sec, *Sigmon and Gibbons*[23]; 9 10^6 cm/sec, *Ryder*[5]

	Drift velocity × 10^6 cm/sec				
T °K	Our results	Duh and Moll [15]	Rodriguez and Nicolet [43]	Costato and Reggiani [41, 42]	Boichenko and Vasetskii [9]
300	9·6	10·5	9·5	10	
245	10·1		10·16 (250°K)	10·9	
200	10·8	11·34	10·73	11·9	
160	11·3		11·6 (150°K)	12·8	
130	11·7			13·5	
110	12		12·45 (115°K)	13·8	
77	12·7	13	13·1	14·2	12·5

The current signal is due to one type of carriers only, namely electrons, and no assumptions need be made on the ratio v_h/v_e of the hole and electron drift velocities and its dependence on the temperature; whereas Duh and Moll[15] had to assume that this ratio was constant and equal to 0·8.

Finally, with our experimental technique no contact injection can affect the measurements.

(b) *Holes*

Figure 7 shows the results obtained for the drift velocity of the holes as a function of the electric field, applied parallel to a ⟨100⟩ crystallographic direction, at several tempera-

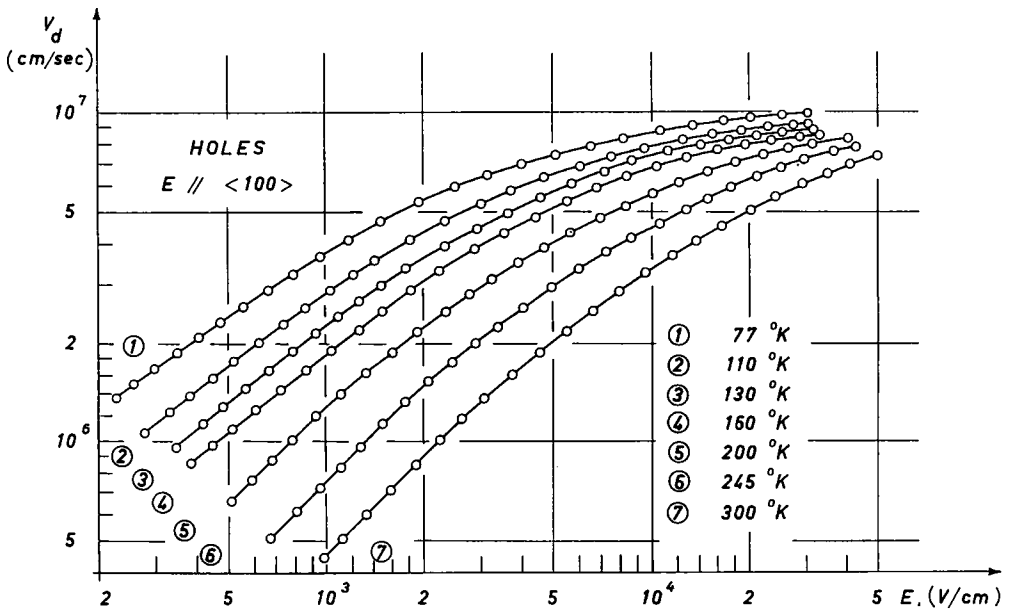

Fig. 7. Hole drift velocity as a function of the electric field parallel to the ⟨100⟩ direction at several temperatures.

tures. At the highest applied electric fields (up to 50 KV/cm) the drift velocity does not reach a limiting value, at any temperature used. Furthermore, for temperatures below 160°K the smallest applied electric fields were not low enough to give the ohmic value of the mobility.

In Figs. 8a, 8b, and 8c the drift velocity data for the holes are shown as functions of the electric field applied parallel to the ⟨111⟩ and ⟨100⟩ directions. To our knowledge, our results[45] give the first clear experimental evidence of an anisotropy effect of holes in silicon in wide ranges of electric fields and temperatures.

A qualitative physical interpretation of our data[39] may be given on the basis of the hot carriers population effect of the multiple warped valence band of silicon, which exhibits a pronounced anisotropy for the upper heavy hole band. Our experimental results support this picture, exhibiting a higher drift

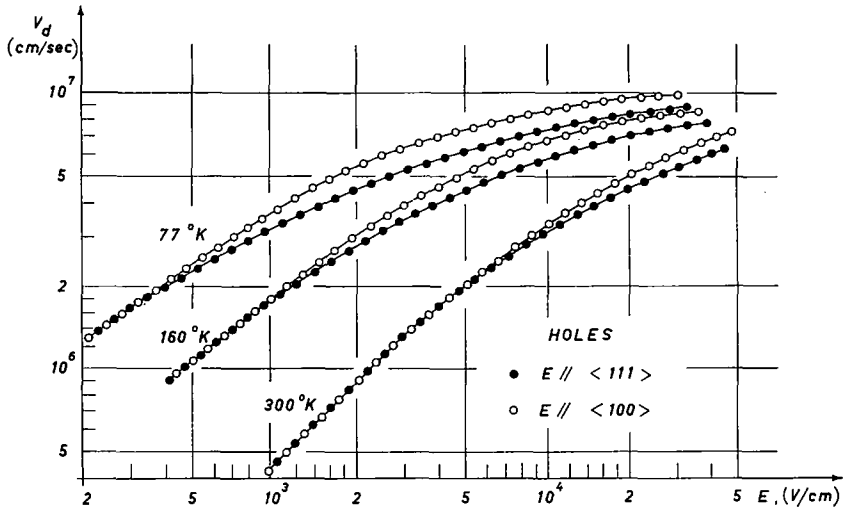

Fig. 8(a)

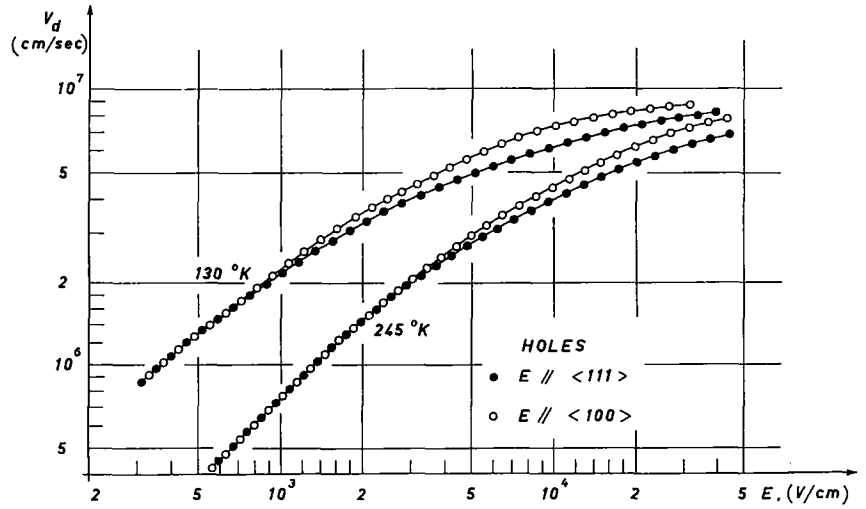

Fig. 8(b)

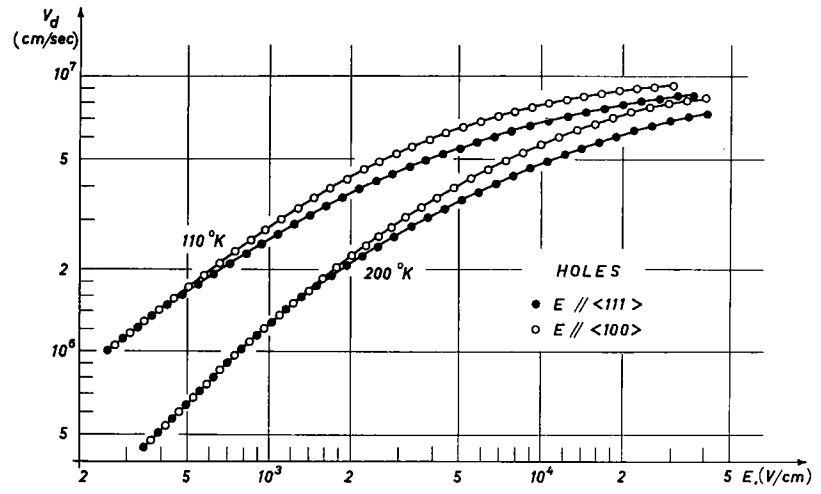

Fig. 8(c)

Figs. 8(a), (b) and (c). Hole drift velocities as functions of the electric field applied parallel to the ⟨111⟩ and ⟨100⟩ directions, at several temperatures.

velocity in the direction of lower effective mass ⟨100⟩ and vice versa ⟨111⟩, in agreement with the anisotropy of the heavy hole band.

In spite of the difficulty of describing the hole drift velocity quantitatively (due to the complex band structure), two important differences between the transport properties of electrons and of holes must be emphasized, both of which contribute to the lower drift velocity of holes than of electrons for a given electric field: (i) Holes have greater effective masses and therefore are less accelerated by the applied field. (ii) The scattering mechanisms responsible for hole drift seem to be more efficient than in the case of electrons [46, 47].

(c) *Comparison of data*

Figure 9 shows a comparison of our experimental results for the drift velocity of electrons (77 and 300°K) and holes (300°K) with the results others have obtained by the time of flight technique and by conductivity measurements. Such comparisons are sometimes difficult, since some authors, because of their experimental technique, report only quantities proportional to the drift velocity [9–11, 14, 15].

The comparison of the electron v_d along the ⟨111⟩ direction at 300°K shows good agreement between our results and those in the literature.

At 77°K the anisotropy effect found by us is only in qualitative agreement with that reported by Asche *et al.*[17]. The lack of quantitative agreement is due to the low value of the low field mobility measured by them.

Data for the hole drift velocity are at 300°K with the electric field parallel to the ⟨111⟩ crystallographic direction.

At electric fields between 40 and 110 KV/cm Rodriguez *et al.*[14] found a saturation drift velocity equal to $7{\cdot}5 \times 10^6$ cm/s ± 5 per cent, in disagreement with the results obtained by Seidel and Sharfetter[10], which show that a saturation drift velocity between 0·96 and $1{\cdot}06 \times 10^7$ cm/s may be obtained with electric fields higher than 2×10^5 V/cm.

Our results show that for electric fields as high as 50 KV/cm no appreciable saturation is obtained for the hole drift velocity.

Recently, Asche *et al.*[48] found an anisotropy effect for the holes at 77°K only in low

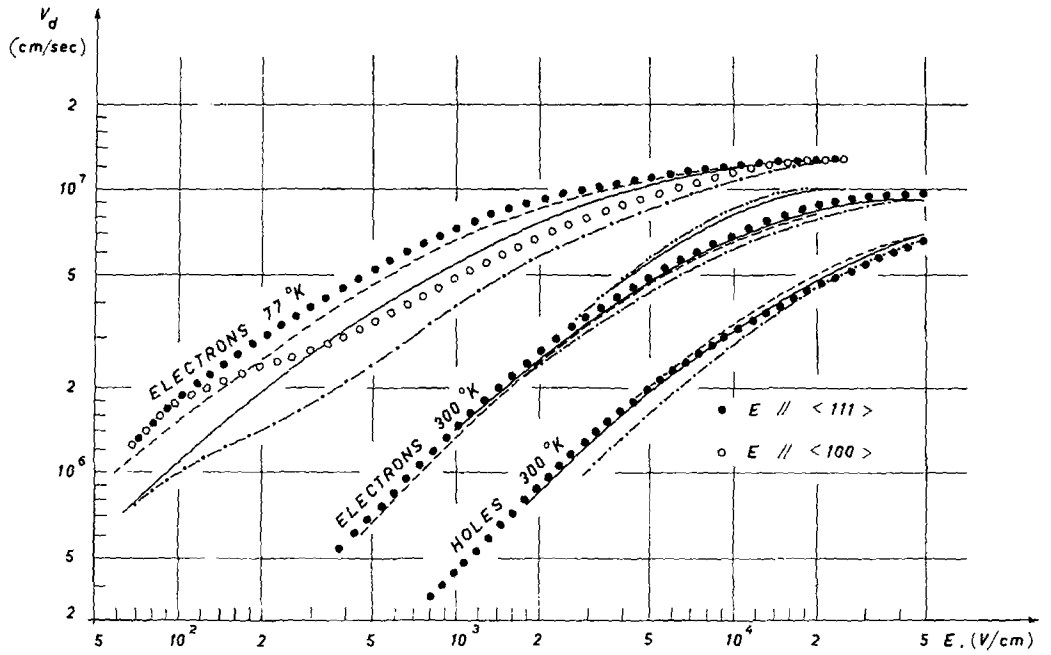

Fig. 9. Comparison between our experimental results on electron and hole drift velocities and the results available in the literature. Electrons $T = 300°K$ $E \| \langle 111 \rangle$, -·-· Rodriguez and Nicolet[43], —— (upper curve Norris and Gibbons[21], —— (lower curve) Sigmon and Gibbons[23], ----- Boichenko and Vasetskii[9], -·- Prior[11]. Electrons $T = 77°K$, ----- Jørgensen *et al.*[16] $E \| \langle 111 \rangle$, —— Asche *et al.*[17] $E \| \langle 111 \rangle$, -·- Asche *et al.*[17] $E \| \langle 100 \rangle$.
Holes $T = 300°K$ $E \| \langle 111 \rangle$, -·-·- Seidel and Scharfetter[10], ----- Norris and Gibbons[21], —— Sigmon and Gibbons[23].

resistivity materials, but according to their results this effect seems to disappear completely in purer samples.

6. CONCLUSIONS

Electron and hole drift velocities have been measured in high purity silicon at several temperatures between 77 and 300°K and for electric fields between 10^2 and 5×10^4 V/cm.

The time of flight technique provides a direct determination of the drift velocity of the carriers by means of space and time measurements. Furthermore, with this technique the drift velocity of both electrons and holes is measured in the same samples.

By using this technique the errors on the measurements have been minimized, as confirmed by the small spread (≤ 5 per cent) of the results obtained in several samples.

The samples were prepared in such a way that the electric field could be applied parallel to both the $\langle 111 \rangle$ and $\langle 100 \rangle$ crystallographic directions. The results obtained showed a clear anisotropy of the electron drift velocity and also, for the first time, of the hole drift velocity.

Furthermore, the electron ohmic mobility (Table 1) and the electron saturation drift velocity (Table 2) have been measured for temperatures between 77 and 300°K. These measurements, performed in high purity samples, are the first made with this technique.

Where possible, our results have been compared with results published by others, and the agreement is generally satisfactory.

The anisotropy effect for the drift velocity of both electrons and holes has been qualitatively interpreted by taking into account the forms of the conduction band and of the valence band of silicon.

Acknowledgements—We are indebted to M. Costato, C. Jacoboni, L. Reggiani, and M. Martini for discussions and suggestions during the course of the work and for constructive criticism of the manuscript. We thank P. Cantoni and M. Bosi for their valuable help in making the measurements.

REFERENCES

1. CONWELL E. M. and WEISSKOPF V. F., *Phys. Rev.* **77**, 388 (1950).
2. SHOCKLEY W., *Bell. Syst. Tech. J.* **30**, 990 (1951).
3. RYDER E. J. and SHOCKLEY W., *Phys. Rev.*, **81**, 139 (1951).
4. CONWELL E. M., *Proc. IRE* **40**, 1331 (1952).
5. RYDER E. J., *Phys. Rev.* **90**, 766 (1953).
6. MORIN F. J., *Phys. Rev.* **93**, 62 (1954).
7. MORIN F. J. and MAITA P. J., *Phys. Rev.* **96**, 28 (1954).
8. GUNN J. B., *J. Electron.* **2**, 259 (1956).
9. BOICHENKO B. L. and VASETSKII V. M., *Soviet Phys. solid State* **7**, 1631 (1966).
10. SEIDEL T. E. and SCHARFETTER D. L., *J. Phys. Chem. Solids* **27**, 1511 (1966).
11. PRIOR A. C., *J. Phys. Chem. Solids* **12** 175 (1959).
12. HAMAGUCHI C. and INUISHI Y. *J. Phys. Chem. Solids* **27** 1511 (1966).
13. DAVIES E. A. and GOSLING D. S., *J. Phys. Chem. Solids* **23** 413 (1962).
14. RODRIGUEZ V., RUEGG H. and NICOLET M-A., *IEEE Trans. on Electron Devices*, **ED-14**, 44(1967).
15. DUH C. Y. and MOLL J. L., *Solid State Electron*, **11**, 917 (1968).
16. JØRGENSEN M. H., MEYER N. I. and SCHMIDT-TIEDMANN K. J., *Proc.* VII *Internat. Conf. Phys. Semicond., Paris*, 457 (1964).
17. ASCHE M., BOITSCHENKO B. L. and SARBEJ O. G., *Phys. Status Solidi* **9**, 323 (1965).
18. McCOMBS A. E., Jr and MILNES A. G., *Int. J. Electron.* **24**, 573 (1968).
19. ALBERIGI QUARANTA A., MARTINI M. and CIPOLLA F., *Phys. Lett.* **17**, No 2, 102 (1965).
20. ALBERIGI QUARANTA A., MARTINI M., OTTAVIANI G., REDAELLI G. and ZANARINI G., *Solid State Electron.* **11**, 685 (1968).
21. NORRIS C. B., Jr and GIBBONS J. F., *IEEE Trans. on Electron Devices*, **ED-14**, 38 (1967).
22. ZULLIGER H. R., NORRIS C. B., SIGMON T. W. and PEHL R. H., *Nucl. Instr. Meth.* **70**, 125 (1969).
23. SIGMON T. W. and GIBBONS J. F., *Appl. Phys. Lett.* **15**, 320 (1969).
24. LANGMANN J. and MEYER O., *Nucl. Instr. Meth.*, **34**, 77 (1965).
25. TOVE P. A., ANDERSSON G., ERICSSON G. and LIDHOLT R., *IEEE Trans. Electron Devices*, **ED-17**, 407 (1970).
26. CAVALLERI G., FABRI G. and SVELTO V., *Nucl. Instr. Meth.* **21**, 177 (1963).
27. TOVE P. A. and SEIBT W., *Nucl. Instr. Meth.* **51**, 261 (1967).
28. TARONI A. and ZANARINI G., *J. Phys. Chem. Solids* **30**, 1861 (1969).
29. MAYER J. W., chap. 5 in "Semiconductor Detectors" (Edited by G. Bertolini and A. Coche) North Holland (1968).
30. RUCH J. G. and KINO G. S., *Phys. Rev.* **174**, 921 (1968).
31. BONCH-BRUEVICH V. L. and LANDSBERG E. G., *Phys. Status Solidi*, **29**, 9 (1968).
32. ALBERIGI QUARANTA A., CANALI C. and OTTAVIANI G., *Rev. Scient Instrum.* **41**, 1205 (1970).
33. PRINCE M., *Phys. Rev.* **93**, 1204 (1954).
34. LONG D., *Phys. Rev.* **120**, 2024 (1960).
35. LOGAN R. A. and PETERS A. J., *J. appl. Phys.* **31**, 122 (1960).
36. PUTLEY E. H. and MITCHELL W. H., *Proc. Phys. Soc.* **A 72**, 193 (1958).
37. LUDWIG G. W. and WATTERS R. L., *Phys. Rev.* **101**, 1699 (1956).
38. COSTATO M. and REGGIANI L., *Phys. Status Solidi* **38**, 665 (1970).
39. CONWELL E. M., *"High Field Transport in Semiconductors"*, Academic Press (1967).
40. COSTATO M. and SCAVO S., *Nuovo Cim.*, **56 B**, 343 (1968).
41. COSTATO M. and REGGIANI L., *Phys. Status Solidi* **42**, 591 (1970).
42. COSTATO M. and REGGIANI L., *Lettere Nuovo Cim.*, **3**, 728 (1970).
43. RODRIGUEZ V. and NICOLET M-A., *J. appl. Phys.* **40**, 496 (1969).
44. CANALI C. and OTTAVIANI G., *Phys. Lett.*, **32A**, 147 (1970).
45. ALBERIGI QUARANTA A., CANALI C. and OTTAVIANI G., *Appl. Phys. Lett.* **16**, 432 (1970).
46. HARRISON W. A., *Phys. Rev.* **104**, 1281 (1956).
47. COSTATO M. and REGGIANI L., *Nuovo Cim.* **B 68**, 64 (1970).
48. ASCHE M., VON BORZESZKOWSKI J. and SARBEJ O. G., *Phys. Status Solidi*, **38**, 357 (1970).